Astronomy & Astrophysics manuscript no. 0281 February 2, 2008
(DOI: will be inserted by hand later)

Abundance difference between components of wide binaries ⋆

S. Desidera[1], R.G. Gratton[1], S. Scuderi[2], R.U. Claudi[1], R. Cosentino,[2,3], M. Barbieri[4], G. Bonanno[2], E. Carretta[1], M. Endl[5], S. Lucatello[1,6], A.F. Martinez Fiorenzano[1,6], and F. Marzari[7]

[1] INAF – Osservatorio Astronomico di Padova, Vicolo dell' Osservatorio 5, I-35122, Padova, Italy
[2] INAF – Osservatorio Astrofisico di Catania, Via S.Sofia 78, Catania, Italy
[3] INAF – Centro Galileo Galiei, Calle Alvarez de Abreu 70, 38700 Santa Cruz de La Palma (TF), Spain
[4] CISAS – Universitá di Padova, Via Venezia 15, Padova, Italy
[5] McDonald Observatory, The University of Texas at Austin, Austin, TX 78712, USA
[6] Dipartimento di Astronomia – Universitá di Padova, Vicolo dell'Osservatorio 2, Padova, Italy
[7] Dipartimento di Fisica – Universitá di Padova, Via Marzolo 8, Padova, Italy

Received 16 Febraury 2004 / Accepted 26 Febraury 2004

Abstract. We present iron abundance analysis for 23 wide binaries with main sequence components in the temperture range 4900-6300 K, taken from the sample of the pairs currently included in the radial velocity planet search on going at the Telescopio Nazionale Galileo (TNG) using the high resolution spectrograph SARG. The use of a line-by-line differential analysis technique between the components of each pair allows us to reach errors of about 0.02 dex in the iron content difference. Most of the pairs have abundance differences lower than 0.02 dex and there are no pairs with differences larger than 0.07 dex. The four cases of differences larger than 0.02 dex may be spurious because of the larger error bars affecting pairs with large temperature difference, cold stars and rotating stars. The pair HD 219542, previously reported by us to have a different composition, here is shown to be normal. For non-rotating stars warmer than 5500 K, characterized by a thinner convective envelope and for which our analyis appears to be of higher accuracy, we are able to exclude in most cases the consuption of more than 1 Earth Mass of iron (about 5 Earth masses of meteoritic material) during the main sequence lifetime of the stars, placing more stringent limits (about 0.4 Earth masses of iron) in five cases of warm stars. This latter limit is similar to the estimates of rocky material accreted by the Sun during its main sequence lifetime. Combining the results of the present analysis with those for the Hyades and Pleiades, we conclude that the hypothesis that pollution by planetary material is the only mechanism responsible for the highest metallicity of the stars with planets may be rejected at more than 99% level of confidence if the incidence of planets in these samples is as high as 8% and similar to the field stars included in current radial velocity surveys. However, the significance of this result drops considerably if the incidence of planets around stars in binary systems and clusters is less than a half of that around normal field stars.

Key words. (Stars:) abundances – (Stars:) planetary systems – (Stars:) binaries: visual – Techniques: spectroscopic

1. Introduction

The evidence for a high metal content in stars harbouring planets is becoming stronger as planet discoveries cumulate and suitable control samples are studied using strictly the same procedures. It appears that the metal abundance of stars with planets is on average about 0.25 dex larger than that of typical control sample stars (Laws et al. 2003) and that the frequency of planets is a strong function of metallicity (Santos et al. 2004, Fischer et al. 2004).

Two alternative hypotheses have been proposed to explain these observations: either the high metallicity is responsible for the presence of planets, making their formation easier; or the planets are the cause of the high metallicity, because of pollution of metal-rich planetary material onto the (outer region of the) central star (Gonzalez 1997).

Infall of planetesimals on the star during the early phases of planet formation is generally expected on the basis of current models of planet formation. The orbital migration proposed to explain the occurrence of the close-in giant planets found by radial velocity surveys also points to the infall on the star of portions of the proto-planetary disk.

Most of the accretion is expected to take place during the early phases of the evolution of the planetary system. However, when a star is still in the phase of gravitational contraction, its convective zone is much thicker than for main sequence stars (see e.g. Murray et al. 2001). In this case, the metal-rich mate-

Send offprint requests to: S. Desidera,
e-mail: desidera@pd.astro.it

⋆ Based on observations made with the Italian Telescopio Nazionale Galileo (TNG) operated on the island of La Palma by the Centro Galileo Galilei of the INAF (Istituto Nazionale di Astrofisica) at the Spanish Observatorio del Roque de los Muchachos of the Instituto de Astrofisica de Canarias

rial should be uniformly distributed by convective mixing over a large portion of the star, resulting in a negligible photospheric chemical alteration even for rather large amounts of accreted material. Late accretion, when the star is approaching or has already reached the main sequence, is likely required to produce observable differences. This may happen due to infall of residual planetesimal/asteroids. The age distribution of the main sequence stars hosting debris disks (Habing et al. 2001), and of the impact craters on Solar System solid bodies, indicate that a significant infall of gas-poor material may be present until 300-400 Myr after star formation; at this epoch the convective zone of a solar-mass star has been thinned enough that significant alterations of the surface abundances may be produced. The ingestion of planets scattered toward the star by dynamical interactions (Marzari & Weidenschilling 2002) might also produce metallicity enhancements at late phases.

The signatures of accretion should be more evident for stars with smaller mixing zones, and disappear for evolved stars, when the outer convective region penetrates deeply into the star. The observations of lithium depletion for stars in the range $1.2 - 1.5\ M_{\odot}$ (the so-called Li-dip, Boesgaard & Tripicco 1986) indicate that an additional mixing mechanism is at work, other than standard convective mixing[1]. It must be further noted that the lithium dip is not present in open clusters as young as Pleiades (Pilachowski et al. 1987), indicating an age dependence. Such an extra-mixing mechanism, besides destroying lithium, should also efficiently flatten the radial abundance profiles of the star, if enrichment of external layers occurred. Therefore the stars that should show the most prominent signatures of accretion are early G-dwarfs and late F-dwarfs, with masses smaller than those in the Li-dip (Murray et al. 2001). The occurrence of 'Li-dip' extra-mixing might also help in explaining the lack of F stars with very high metallicity ([Fe/H]> +0.50), predicted by the pollution scenario when considering only the extension of the convective zone.

The metal abundance of planet hosts does not appear to be correlated with the thickness of the convective zone (Pinsonneault et al. 2001, Santos et al. 2004). This seems to indicate that pollution is not the most relevant contribution to the high metallicity of stars with planets. On the other hand, two possible effects might in principle explain such a lack of a trend as a function of the thickness of the convective envelope. The first is the result of Vauclair (2004), who suggests that, when the metallicity difference between the inner and outer parts of a star exceedes a threshold, further mixing is induced in the transition zone, therefore diluting the atmospheric metallicty enhancement. The second effect can be considered if the metal enrichment is dominated by the ingestion of already formed planets. According to the hydrodynamical simulations by Sandquist et al. (1998), a $1.22\ M_{\odot}$ star should be able to only partially consume an engulfed giant planet within its thin convective zone. Depending on the actual distribution of heavy elements within the planet (possibly mostly confined in the planet core), the resulting alteration of chemical composition might be even smaller than for a solar-like star that is able to consume nearly completely a Jupiter-like planet within its convective zone.

On the other hand, several observational results support the occurrence of pollution phenomena.

Smith et al. (2001) found indications of systematic element-to-element differences as a function of the condensation temperature on some planet host stars. This could be explained by the infall of material devoid of light elements, such as rocky planets or asteroids. However, such chemical composition trends can be confused with galactic chemical evolution trends, and can be more easily studied in binaries and clusters. Gratton et al. (2001b), hereafter Paper I, performed a differential analysis of 6 visual main sequence binaries. They found one pair (HD 219542) with a 0.09 dex iron content difference, four pairs with very similar composition and one ambiguous case (HD 200466). Laws & Gonzalez (2001) also found a small difference between the components of 16 Cyg. A similar approach can be pursued to look for chemical anomalies among open cluster stars. Paulson et al. (2003) studied 55 FGK dwarfs in the Hyades. They found two stars with abundances 0.2 dex larger than the cluster mean, but their membership is questionable. The Pleiades were studied by Wilden et al. (2002); they found one possible candidate out of 15 stars with abundance 0.1 dex above the cluster mean and very little scatter for the other stars (0.02 dex). No correlation appears to be present between iron and lithium abundances.

The presence of ^{6}Li might be a strong indication of accretion phenomena, since this element is easily destroyed and cannot be observed in main sequence stars unless recently fallen onto the star from an external source. The presence of ^{6}Li in HD 82943 is controversial (Reddy et al. 2002, Israelian et al. 2003). If confirmed, this would indicate the infall of a giant planet. Anomalies of the most abundant ^{7}Li isotope are instead easier to find (see e.g. Pasquini et al. 1997, King et al. 1997, Martin et al. 2002) but they are more difficult to interpret as they might not be linked to planetary pollution.

Murray et al. (2001) found that the Sun should have ingested some $2\ M_{\oplus}$ of meteoritic material (about $0.4\ M_{\oplus}$ of iron), considering the drop of iron density in the asteroid region and the time distribution of the impact craters. This corresponds to a metallicity enhancement of 0.017 dex. Helioseismology currently does not allow a confirmation of the presence of such a small metal abundance difference between the inner and the outer regions (Winnick et al. 2002), with upper limits on the amount of accreted iron about four times higher than the Murray et al. (2001) estimate[2].

From this discussion, it appears that the comparison of the chemical composition of wide binaries is a very powerful approach to study the occurrence of planetary pollution. The number of pairs studied in Paper I is too small to allow significant inferences about the frequency and the amount of

[1] Alternative explanations of Li-dip depletion such as mass loss or gravitational sedimentation do not seem to be supported by observations, see Do Nascimento et al. (2000).

[2] The comparison between the results quoted in the original papers show some inconsistencies because of different assumptions on the composition of meteoritic material. In this paper, we adopt the meteoritic abundances by Lodders (2003). The mass fraction of iron is thus 18.3% of the meteoritic material.

chemical anomalies in visual binaries. In this paper, we significantly enlarge the number of pairs studied (23), with various improvements in the analysis procedure. We will then combine the results of the present analysis with the literature results for Hyades and Pleaides, to draw tentative conclusions about the impact of planetary material pollution.

2. Observations and data reduction

A radial velocity survey aimed to find planets around stars in wide binaries is on-going at TNG (the Italian Telescopio Nazionale Galileo on La Palms, Canary Islands, Spain) using the high resolution spectrograph SARG (Gratton et al. 2001a). The goals of the project are the study of the dynamical effects due to the presence of the companion on the existence and orbital characteristics of planetary systems, and the study of chemical composition differences possibly caused by the ingestion of planetary material. A recent report describing the status of the survey is given by Gratton et al. (2004).

The radial velocities are determined using the iodine cell technique. A high resolution, high quality spectrum of each star, free of iodine lines, is used as template for the radial velocity analysis. Such observational material is fully suited for a careful abundance analysis, without further observational efforts. All the spectra were acquired with the Yellow Grism, that covers the spectral range 4600-7900 Å without gaps, and the 0.25 arcsec slit. The resulting resolution is R=150000 (2 pixel sampling). The insertion of a suitable filter avoids any grism second order contamination in the red extreme of the spectra. During the observations, the slit was usually oriented perpendicularly to the separation of the components to minimize the contamination of the spectra by the companion.

We present in this paper the stellar templates acquired between June 2001 and November 2002. We also reanalyzed the pairs included in Paper I to take into account the modifications in our analysis procedure. The spectra were reduced in the standard way using IRAF[3]. The signal to noise ratio per pixel in most cases exceeds 150.

3. Abundance analysis

The analysis procedure is similar to that performed in Paper I, with some differences outlined in detail below. The unidimensional spectra were analyzed using routines within the ISA code (Gratton 1988). The continuum level was determined by fitting a cubic spline through automatically selected regions of the spectra, excluding discrepant points identified by eye. Then the equivalent widths (EWs) were measured using an automatic procedure, that estimates a local continuum level and perform a Gaussian fit to the selected lines (see Bragaglia et al. 2001 for details)[4]. The assumption of a Gaussian line profile fails for stars with rotational velocities larger than about 5-10 km/s (at the very high resolution of our spectra the contribution of instrument profile becomes small). The resulting EWs

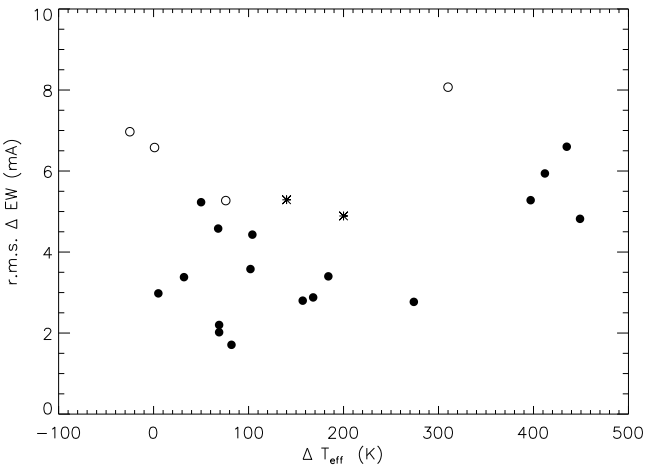

Fig. 1. r.m.s scatter in equivalent width differences ΔEW between the components of the binaries analyzed in this paper as a function of temperature difference ΔT_{eff}. Open circles represent stars with rotational broadening larger than about 5 km/s, filled circles slowly rotating stars, asterisks the two pairs with slightly evolved primaries.

are overestimated for these stars. We then apply a suitable correction, determined from spectral synthesis of stars with different rotational velocities, to the EWs of stars with $v \sin i$ larger than 5 km/s (HD 8071 A/B, BD+231978A/B, HD 108574/5, HD 216122A/B).

The line list is the same used in Paper I, with the addition of some vanadium lines from Whaling et al. (1985).

The errors of EWs can be estimated by the rms of the difference of EWs between the components of pairs whose temperatures differ by less than 200 K, about 2-3 mÅ (Fig. 1). Stars that have significant rotation have larger errors. The increase of the rms of the difference for stars with larger temperature difference and for the pairs whose primary appears to be evolved out of the main sequence may be explained by the intrinsic variations of the line-by-line sensitivity to temperature and gravity changes. The signal to noise ratio seems to play a role in EW errors only for the few spectra with S/N lower than about 100-120.

The abundance analysis made use of Kurucz (1995) model atmospheres, computed with the overshooting option switched off (Castelli et al. 1997). The primaries were analyzed differentialy with respect to the Sun, then the line-by-line abundance differences between primaries and secondaries were determined.

Improvements with respect to Paper I concern the inclusion of the damping wings in the analysis of lines with $\log(EW/\lambda) > -5.4$ (in the previous analysis this limit was fixed to –5.1). The calculation of the damping constant is based on the formalism by Barklem et al. (2000), while in Paper I we used an enhancement factor to the Unsold formula (Unsold 1955). These improvements allow a more appropriate treatement of microturbulence (fixed to 0 in Paper I) and an extension toward stronger lines (up to 100 mÅ), while in Paper I we limited ourselves to EWs < 50 mÅ. The line list is then expanded by about 50%. To

[3] IRAF is distributed by the National Optical Observatory, which is operated by the Association of Universities for Research in Astronomy, Inc., under contract with the National Science Fundation

[4] The equivalent widths will be made available in electronic form.

remove outliers, we also used an automathic procedure that iteratively cleans the set of lines, disregarding outliers that yield abundances differing more than 2.5 σ from the average abundance of the remaining lines, while in Paper I outliers were removed by hand.

3.1. Analysis of Primaries

Table 1 reports visual and absolute magnitudes, *B-V* colours, parallaxes, masses and projected separations for the program stars. *V* band magnitudes are the weighted average of Tycho and Hipparcos photometries (ESA 1997), corrected to the standard system using the calibrations by Bessell (2000). *B-V* colours are from Tycho and corrected using Bessell (2000). The parallaxes are from Hipparcos. When separate parallaxes were available for the two components (HD 108574/5, HD 135101 A and B), a weighted average was performed. The absolute magnitudes were corrected by the Lutz-Kelker effect following Hanson (1979). The differences with respect to Paper I concern the inclusion of the Hipparcos photometry in the calculation of magnitude differences, the correction to the standard system of the Tycho photometry, the inclusion of some further literature measurements, and the application of the Lutz-Kelker correction to parallaxes.

The stellar masses were determined from the isochrones of Girardi et al. (2002), averaging the masses obtained for 1 Gyr main sequence stars having absolute magnitudes and temperatures equal to those of the program stars for the appropriate metallicity[5]. To take into account the dependences on temperature and metallicity, the masses were determined iteratively during the abundance analysis. For the stars that show significant evolution out of the main sequence (namely HD 135101A and HD 19440A), stellar masses were taken from the suitable isochrone that fits the position of the components on the color-magnitude diagram. In Paper I the mass were derived using Tycho colours instead of the derived temperatures (coupled with absolute magnitudes) and using Gray (1992) tables (therefore neglecting metallicty effects).

Table 2 summarizes the magnitude differences for program stars, including Hipparcos, Tycho and further ground-based photometry when available. Only literature observations reported in the standard system are included. When available, we used the internal errors as estimate of errors. A 0.04 mag error was assigned to the Docobo et al. (2000) magnitudes from the scatter of magnitude difference of pairs with multiple observations; a 0.02 mag error was assigned to the Simbad photometry of HD 108575/5 and HD 135101 and to the Carney et al. (1994) photometry of HD 200466. The adopted magnitude difference is the weighted average of individual determinations. The resulting error is lower than 0.02 mag in most cases.

There is an offset of 0.052 ± 0.016 mag (rms 0.075 mag) between Hipparcos and Tycho magnitude differences. The discrepancy is larger for pairs with a magnitude difference larger than 0.65 mag. There is instead no significant offset between Hipparcos and the literature determinations: the mean offset is 0.005 ± 0.007 mag (rms 0.023 mag). The lower quality of Tycho photometry is also supported by the very large difference of temperatures derived from *B-V* Tycho colors with those derived from spectroscopy (see Table 5).

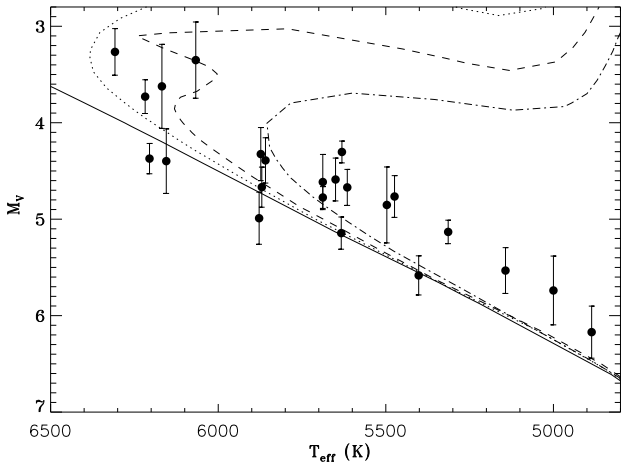

Fig. 2. Color-Magnitude diagram for primaries using Hipparcos and Tycho magnitudes (corrected to the standard system using Bessell 2000) with Hipparcos parallaxes and our spectroscopically determined effective temperatures. The solar metallicity isochrones by Girardi et al. (2002) are overplotted for ages of 1, 2.5, 4 and 8 Gyr.

The dispersion of Hipparcos and literature differences suggests that quoted errors are underestimated by about 30%. This may be due to the fact that in most cases the two components are not resolved by Hipparcos. The Hipparcos epoch photometry (composite magnitudes) shows a scatter larger than internal errors in many cases (flag 'Duplicity induced variability'). Uncertainties in the transformation to the standard system, based on Tycho colors, may also play a role. We include such 30% increase of errors in our adopted error bars.

As in Paper I, effective temperatures were determined from the ionization equilibrium. This method gives robust values for the differences between the temperatures of the two components, since in this case uncertainties in the absolute magnitude (the largest contribution to errors) cancel out, the two components being virtually at the same distance from the Sun. Note however that errors are much larger for the analysis with respect to the Sun (analysis of primaries), since in this case the full error bar in the parallax must be taken into account.

In this paper, we also use vanadium lines, characterized by a temperature sensitivity larger than typical of an iron line. The lack of a suitable number of VII lines forced us to compare VI to FeII. Intrinsic differences of [V/Fe] might in principle introduce spurious effects on our temperatures. However, vanadium is not known to show peculiar relative abundance with respect to iron for both Population I and Population II stars (Gratton & Sneden 1991). Possible small intrinsic abundance differences due to chemical evolution are not of concern in the differential analysis of the binary components. Spurious effects due to accretion of chemically fractionated material, more crucial for the

[5] The periods of the observed systems are too long for any reliable determination of dynamical masses (see Desidera et al. 2003 for the case of HD 219542).

Table 1. Visual and absolute magnitudes, B-V color, Hipparcos parallaxes, stellar masses (derived iterativey during the abundance analysis using the spectroscopic temperatures and abundances) and projected binary separation for program stars. As discussed in the text, the formal errors on magnitudes and colors are likely underestimated.

Object	V_A	V_B	$(B-V)_A$	$(B-V)_B$	π mas	$M_{V(A)}$	$M_{V(B)}$	M_A $M_\odot$	M_B $M_\odot$	ρ $''$	ρ AU
HD 8009	8.819 ± 0.007	9.724 ± 0.017	0.64 ± 0.03	0.82 ± 0.07	15.43±2.02	4.61±0.29	5.52±0.29	0.95	0.85	4.7	326
HD 8071	7.312 ± 0.003	7.573 ± 0.004	0.58 ± 0.01	0.60 ± 0.01	19.67±1.58	3.73±0.17	3.99±0.17	1.25	1.22	2.2	115
HD 9911	9.428 ± 0.008	9.448 ± 0.008	0.90 ± 0.04	0.89 ± 0.04	20.40±3.32	5.74±0.36	5.76±0.36	0.85	0.85	3.9	213
HD 13357	8.180 ± 0.006	8.647 ± 0.010	0.67 ± 0.03	0.73 ± 0.05	20.41±1.75	4.67±0.19	5.14±0.19	0.98	0.93	5.9	297
HD 17159	8.775 ± 0.007	8.923 ± 0.007	0.54 ± 0.03	0.53 ± 0.03	14.65±2.24	4.40±0.33	4.55±0.33	1.15	1.12	2.7	203
HD 19440	7.874 ± 0.004	8.574 ± 0.007	0.47 ± 0.01	0.53 ± 0.02	12.55±1.39	3.27±0.24	3.96±0.24	1.25	1.14	6.0	501
HD 30101	8.782 ± 0.009	8.848 ± 0.009	0.82 ± 0.04	0.91 ± 0.03	23.43±2.55	5.53±0.24	5.66±0.24	0.84	0.83	4.6	205
HD 33334	8.023 ± 0.004	8.857 ± 0.009	0.70 ± 0.03	0.80 ± 0.07	21.39±2.18	4.59±0.22	5.42±0.22	1.00	0.89	4.7	229
HD 66491	9.253 ± 0.009	9.312 ± 0.009	0.75 ± 0.05	0.67 ± 0.05	15.11±2.71	4.85±0.39	4.91±0.39	0.96	0.96	5.1	387
BD+23 1978	9.395 ± 0.010	9.530 ± 0.011	0.80 ± 0.06	0.75 ± 0.05	24.04±2.97	6.17±0.27	6.31±0.27	0.84	0.84	2.6	115
HD 106515	7.960 ± 0.005	8.234 ± 0.007	0.79 ± 0.02	0.83 ± 0.03	27.50±1.54	5.13±0.12	5.41±0.12	0.93	0.89	7.0	257
HD 108574/5	7.418 ± 0.005	7.972 ± 0.007	0.56 ± 0.01	0.67 ± 0.02	25.06±1.81	4.37±0.16	4.93±0.16	1.22	1.11	9.8	399
HD 123963	8.758 ± 0.006	9.511 ± 0.010	0.60 ± 0.03	0.54 ± 0.04	13.81±1.74	4.33±0.28	5.08±0.28	1.08	0.96	2.6	200
HD 132563	8.966 ± 0.007	9.472 ± 0.010	0.54 ± 0.03	0.57 ± 0.05	10.15±2.01	3.62±0.44	4.13±0.44	1.13	1.06	4.2	491
HD 132844	9.022 ± 0.006	9.114 ± 0.007	0.55 ± 0.05	0.63 ± 0.05	16.57±2.05	4.99±0.27	5.08±0.27	1.01	0.99	3.0	192
HD 135101	6.656 ± 0.006	7.500 ± 0.009	0.69 ± 0.01	0.75 ± 0.02	34.18±1.78	4.30±0.11	5.15±0.11	0.97	0.95	23.5	694
HD 190042	8.755 ± 0.009	8.778 ± 0.006	0.73 ± 0.03	0.80 ± 0.04	16.52±1.64	4.76±0.22	4.79±0.22	0.96	0.94	4.2	264
HD 200466	8.399 ± 0.005	8.528 ± 0.006	0.71 ± 0.02	0.79 ± 0.03	22.83±1.75	5.14±0.17	5.28±0.17	0.99	0.97	4.7	210
HIP 104687	8.144 ± 0.006	8.189 ± 0.006	0.64 ± 0.06	0.71 ± 0.06	20.87±1.99	4.67±0.21	4.72±0.21	1.09	1.08	4.0	198
HD 213013	8.982 ± 0.008	9.612 ± 0.013	0.81 ± 0.04	0.93 ± 0.08	21.59±2.01	5.58±0.20	6.21±0.20	0.93	0.84	5.5	263
HD 215812	7.275 ± 0.005	7.576 ± 0.006	0.64 ± 0.02	0.70 ± 0.02	31.94±1.66	4.78±0.11	5.08±0.11	0.95	0.92	2.2	70
HD 216122	8.062 ± 0.011	8.186 ± 0.013	0.58 ± 0.02	0.58 ± 0.03	13.11±2.36	3.35±0.40	3.47±0.40	1.23	1.22	5.3	464
HD 219542	8.174 ± 0.006	8.547 ± 0.008	0.64 ± 0.03	0.71 ± 0.04	18.30±1.97	4.39±0.23	4.78±0.23	1.08	1.05	5.3	303

goals of this work, are also not expected, since iron and vanadium have very similar condensation temperatures (1334 and 1429 K respectively, according to Lodders 2003). The hyperfine splitting of V lines is included in our analysis as in Gratton et al. (2003). For the few lines for which the hyperfine splitting constants are not available, a correction was applied considering the abundance difference of the other lines due to hyperfine splitting as a function of EW.

For the line lists we are using, the sensitivity of FeI-FeII and VI-FeII differences on temperature is about 0.0009 and 0.0015 dex/K respectively. Temperatures from iron and vanadium were averaged.

Stellar gravities were calculated using the standard relation

$$\log g = \text{const} + \log M + 0.4\,(M_V + BC) + 4\log T_{\rm eff} \qquad (1)$$

where the constant term includes the solar quantities. We used the absolute magnitudes from Hipparcos parallaxes, the stellar masses determined from the isochrones of Girardi et al. (2002) and the bolometric corrections by Kurucz (1995). Since the derived masses and gravities depend on temperatures and metallicities, an iterative procedure is required.

The errors in the absolute magnitudes of the primaries are typically 0.2-0.3 mag. These propagate into errors of about 0.10 dex in $\log g$, therefore significantly affecting the derived temperature from the ionization equilibrium (±30 K) and the abundances for the primaries (±0.04 dex)[6]. However, such sources of error are not of concern for the differential analysis between primaries and secondaries, where they cancel out. Only errors in relative photometry (less than 0.05 mag in all but one case) play a role in this case.

Microturbulent velocity was originally fixed by eliminating trends of Fe I abundance with expected equivalent width (see Magain 1984). Residual trends with expected equivalent width are often present for cool stars ($T_{\rm eff}$ <5300 K), even when the microturbulent velocity was set at zero. These residual trends may be due to various causes, the most likely being an incorrect (too large) temperature gradient of the adopted model atmospheres. To reduce the impact of this effect on our differential abundance analyses, in these cases we only considered weak lines, that form deeper in the atmosphere.

As expected for main sequence stars, there is a relation between the temperature and the microturbulence derived as a free parameter from the analysis (Fig. 3). The residuals with respect to a global fitting to the temperature-microturbulence relation (excluding rotating stars and the two slightly evolved stars) show a dispersion of 0.22 km/s. This is comparable to the errors in determination of individual values of microturbulence, estimated to be about 0.2 km/s. Since the scatter around the fitting relation appears to be dominated by measurement errors, we adopted the values given by the relation (shown in Fig. 3), iterating the process if the analysis with the revised microturbulence values requires some temperature and abundance changes.

For the evolved stars HD 135101A and HD 19440A we instead adopted the values of microturbulence resulting from the stellar analysis (as expected they are larger than the standard relation by 0.25 and 0.10 km/s respectively).

Table 3 summarizes the atmospheric parameters adopted in the abundance analysis. Table 4 shows the results of the analysis of the primaries.

[6] In the case of HD 132844A the procedure used for the other stars gives very high gravities ($\log g$ = 4.74), This is likely due to a large error in parallaxes. For this star only, the analysis of the primary was purely spectroscopic, with the temperature derived from the excitation equilibrium and gravity from the ionization equilibrium.

Table 2. Magnitude difference for program stars.

Object	ΔV Hipparcos	ΔV Tycho	ΔV Other	Ref. Other	ΔV Adopted
HD 8009	0.935±0.021	0.763±0.046			0.905±0.065
HD 8071	0.281±0.006	0.233±0.010			0.268±0.021
HD 9911	0.026±0.013	-0.023±0.033			0.019±0.017
HD 13357	0.465±0.013	0.477±0.034	0.47±0.01	1	0.469±0.010
HD 17159	0.148±0.011	0.166±0.028			0.150±0.010
HD 19440	0.710±0.008	0.631±0.021	0.68 ± 0.01	1	0.692±0.016
HD 30101	0.134±0.013	-0.153±0.032	0.146±0.005	2	0.134±0.025
			0.13±0.01	1	
HD 33334	0.839±0.010	0.700±0.048	0.82±0.01	1	0.827±0.015
HD 66491	0.057±0.013	0.077±0.047			0.058±0.016
BD+23 1978	0.139±0.016	0.092±0.041			0.132±0.019
HD 106515	0.273±0.009	0.263±0.024			0.272±0.011
HD 108574/5	0.554±0.012	0.572±0.015	0.57	3	0.563±0.011
HD 123963	0.773±0.013	0.664±0.034			0.759±0.036
HD 132563	0.511±0.013	0.451±0.039			0.505±0.018
HD 132844	0.095±0.009	0.027±0.044			0.092±0.013
HD 135101	0.894±0.020	0.833±0.012	0.85	3	0.849±0.017
HD 190042	0.021±0.008	0.037±0.031			0.022±0.010
HD 200466	0.133±0.008	0.101±0.021	0.15 ± 0.01	1	0.139±0.009
			0.17	4	
HIP 104687	0.048±0.008	-0.052±0.053	0.00	5	0.045±0.010
			0.06	5	
HD 213013	0.631±0.016	0.627±0.047	0.62	5	0.628±0.017
			0.62	5	
HD 215812	0.307±0.008	0.243±0.019			0.297±0.022
HD 216122	0.123±0.011	0.123±0.024	0.11 ± 0.01	1	0.117±0.009
HD 219542	0.369±0.010	0.412±0.034	0.391±0.007	2	0.387±0.006

References: 1: Nakos et al. (1995); 2: Cuypers & Seggewiss (1999); 3: Simbad; 4: Carney et al. (1994); 5: Docobo et al. (2000)

Table 3. Adopted atmospheric parameters.

Object	$T_{eff(A)}$	$T_{eff(B)}$	$\log g_A$	$\log g_B$	$[A/H]_A$	$[A/H]_B$	ξ_A	ξ_B
HD 8009	5688	5291	4.30	4.45	–0.20	–0.14	0.75	0.00
HD 8071	6218	6142	4.24	4.32	+0.26	+0.26	1.10	1.10
HD 9911	5000	4968	4.40	4.39	+0.06	+0.01	0.00	0.00
HD 13357	5615	5341	4.31	4.36	–0.02	–0.01	0.65	0.25
HD 17159	6155	6051	4.46	4.48	+0.02	+0.02	1.10	1.00
HD 19440	6308	6108	4.09	4.27	–0.05	–0.05	1.25	1.05
HD 30101	5143	5061	4.39	4.39	–0.14	–0.14	0.00	0.00
HD 33334	5650	5201	4.30	4.39	+0.02	+0.03	0.70	0.00
HD 66491	5497	5492	4.33	4.35	+0.03	+0.02	0.55	0.55
BD+23 1978	4886	4911	4.51	4.58	+0.22	+0.22	0.00	0.00
HD 106515	5314	5157	4.35	4.37	+0.08	+0.07	0.10	0.00
HD 108574/5	6205	5895	4.49	4.55	+0.23	+0.23	1.10	0.90
HD 123963	5873	5438	4.31	4.39	+0.11	+0.14	0.90	0.45
HD 132563	6168	5985	4.15	4.27	–0.18	–0.19	1.10	0.95
HD 132844	5878	5809	4.12	4.13	–0.18	–0.18	0.90	0.85
HD 135101	5631	5491	4.17	4.44	+0.05	+0.05	0.95	0.55
HD 190042	5474	5406	4.28	4.26	+0.02	+0.02	0.50	0.40
HD 200466	5633	5583	4.51	4.54	+0.06	+0.04	0.70	0.65
HIP 104687	5870	5801	4.45	4.44	+0.11	+0.12	0.90	0.85
HD 213013	5402	4990	4.56	4.58	+0.08	+0.07	0.40	0.00
HD 215812	5688	5586	4.37	4.43	–0.19	–0.21	0.75	0.65
HD 216122	6067	6066	4.04	4.09	+0.25	+0.28	1.05	1.05
HD 219542	5859	5691	4.34	4.42	+0.14	+0.14	0.90	0.75

Table 4. Results of abundance analysis for primaries.

Object	[Fe/H]I	rms	N_{lines}	[Fe/H]II	rms	N_{lines}	[V/H]I	rms	N_{lines}
HD 8009	–0.195	0.084	126	–0.194	0.164	32	–0.195	0.113	28
HD 8071	+0.267	0.133	133	+0.203	0.197	30	+0.085	0.117	12
HD 9911	+0.058	0.082	73	+0.099	0.151	20	+0.177	0.162	27
HD 13357	–0.012	0.130	146	–0.045	0.094	28	–0.109	0.090	32
HD 17159	+0.017	0.104	126	+0.038	0.129	33	+0.068	0.165	20
HD 19440	–0.058	0.111	138	–0.038	0.152	34	–0.003	0.158	22
HD 30101	–0.148	0.079	104	–0.174	0.095	26	–0.229	0.083	25
HD 33334	+0.015	0.078	122	+0.012	0.174	34	+0.013	0.108	32
HD 66491	+0.031	0.079	125	+0.016	0.130	25	–0.013	0.118	30
BD+23 1978	+0.221	0.171	60	+0.282	0.157	14	+0.367	0.150	11
HD 106515	+0.078	0.065	85	+0.094	0.090	25	+0.120	0.092	23
HD 108574/5	+0.214	0.120	128	+0.259	0.198	28	+0.332	0.218	24
HD 123963	+0.111	0.086	140	+0.075	0.102	33	+0.010	0.091	28
HD 132563	–0.185	0.103	139	–0.186	0.109	34	–0.197	0.173	19
HD 132844	–0.182	0.077	130	–0.208	0.153	32	–0.249	0.059	23
HD 135101	+0.068	0.073	136	+0.077	0.125	31	+0.094	0.121	31
HD 190042	+0.045	0.092	130	+0.036	0.074	23	+0.019	0.143	31
HD 200466	+0.050	0.061	82	+0.055	0.137	30	+0.060	0.084	29
HIP 104687	+0.123	0.083	126	+0.106	0.157	31	+0.075	0.103	26
HD 213013	+0.084	0.088	84	+0.112	0.144	26	+0.151	0.129	30
HD 215812	–0.195	0.083	136	–0.198	0.074	29	–0.204	0.094	27
HD 216122	+0.263	0.116	124	+0.263	0.141	23	+0.269	0.159	20
HD 219542	+0.135	0.084	132	+0.122	0.109	27	+0.102	0.143	28

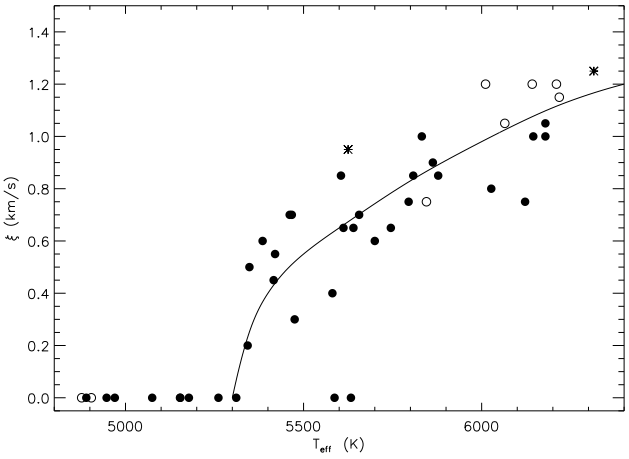

Fig. 3. Microturbulence as a function of effective temperature resulting from the analysis performed leaving the microturbulence as a free parameter. Symbols as in Fig. 1. The relation between temperature and microturbulence adopted in the analysis is shown as a continuous line.

3.2. Differential analysis of secondaries

The secondary of each pair was analyzed differentially with respect to the primary, using strictly the same line set. The initial line list for the differential analysis includes the lines not removed as outliers in the analysis of both components. Further iterative clipping is performed to exclude lines that gives abundance differences outside $\pm 2.5\sigma$ with respect to the average of the other lines.

The differential approach allows us to remove a number of possible systematic errors in the analysis, as indicated by the internal scatter of abundance difference that is lower than expected if the errors of the two components were fully independent (Fig. 4). The degree of correlation between the abundances obtained from individual lines on the spectra of the two components is a function of the difference of the temperature of the stars: we found that the correlation is negligible when this difference is larger than about 300 K. This is likely due to the combination of two factors: (i) for large temperature differences, line strengths are very different, due to the different impact of continuum opacity; and (ii) systematic errors in the determination of the correct continuum level become quite different. It is clear that the differential analysis yields most accurate results when the two components are very similar.

Table 5 shows the temperature differences given by different methods.

The first and second column give the temperature difference from the ionization equilibrium of iron and vanadium respectively and the third column their weighted average. As shown in Fig. 5, for the pairs with temperature of the secondary larger than 5450 K and excluding the rotating stars characterized by much larger error bars, iron and vanadium temperatures agree very well (mean offset -3 ± 7 K, rms 25 K, 10 pairs). A possible trend in the sense of vanadium giving larger temperatures differences may be present for the stars in the range 5100-5450 K, while the situation is less clear for even cooler stars. Systematic trends in cooler stars may be caused by some residual effects of hyperfine splitting or to the fact that most of the lines in our line list become quite strong in the spectra of these stars, for which a trend of abundance as a function of EWs still remains

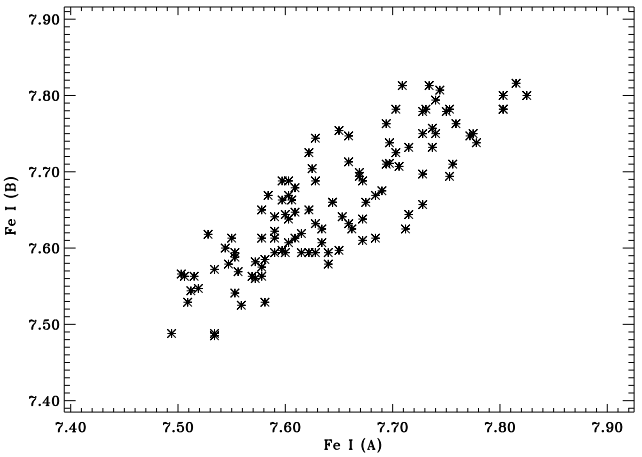

Fig. 4. Iron abundance derived for each line for the components of HIP 104687 A and B. A clear correlation is present, indicating that the use of a line-by-line differential analysis significantly reduces the errors on abundance difference between the components.

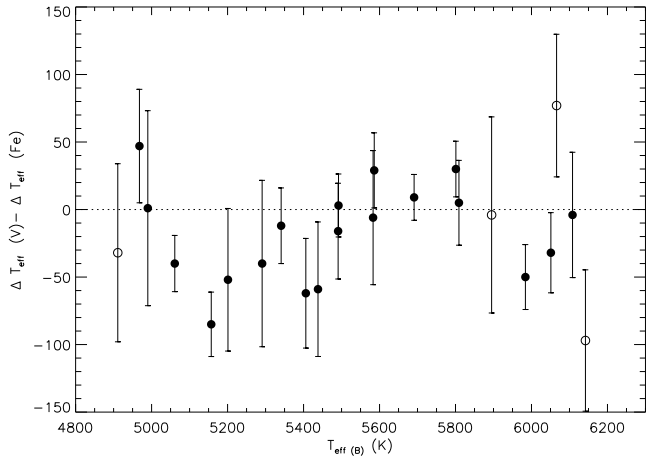

Fig. 5. Differences between the temperatures derived using the iron and vanadium lines as a function of the temperature of the secondary.

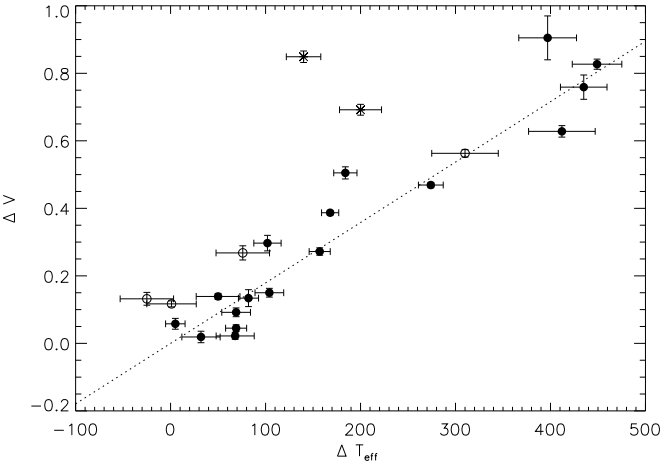

Fig. 6. Magnitude vs temperature differences. The dotted line represents the typical slope alone the main sequence of a 1 Gyr solar metallicity isochrone. Symbols as in Fig. 1. The two discrepant cases are HD 135101 and HD 19440, that have primaries clearly evolved off of the main sequence.

for such cool stars, as discussed above. A better evaluation of the existence of systematic trends is postponed to the analysis of further stars for which spectra already have been obtained.

The excitation temperatures show an offset of 24 ± 14 K (rms 59 K) for the 19 slow rotating pairs with respect to temperatures based on ionization equlibrium. The residual slopes of abundance difference as a function of excitation potential are correlated with those as a function of equivalent width, suggesting a common origin (likely the inadequacies of the atmospheric models and/or a possible underestimate of equivalent widths of strong lines when using a Gaussian fit). Therefore, the internal errors on the excitation temperature should not represent the full error bar.

Temperature differences from colors are calculated using the calibrations by Alonso et al. (1996). B-V colors are taken from Table 1. V-I of HD 30101 and HD 219542 are from Cuypers & Seggewiss (1999) and those of HD 108584/5 and HD 135101 are from the Hipparcos Catalog. Transformation to the Johnson photometric system was performed following Bessell (1983). 2MASS photometry was transformed to the TCS photometric system using the calibrations provided by Cutri et al. (2003) and those by Alonso et al. (1994). The only pair for which Strömgren photometry is available for both components is HD 135101 (Hauck & Mermilliod 1998). A temperature difference of 160 K is derived. It appears that temperatures based on colors have typically very poor precision, likely because of the photometric errors induced by the small separation of the components.

The temperature difference from ΔV is estimated considering the slope of the main sequence on the 1 Gyr solar metallicity isochrone. It does not include evolutionary effects and therefore represents an upper limit to the actual temperature difference.

When considering the differential analysis between the two components, parallaxes no longer play a role; the same applies to absolute errors on mass estimates. Only errors on relative photometry are relevant. The errors on magnitude difference are less than 0.05 mag in all but one case (HD 8009). A 0.05 mag error in magnitude difference produces errors for relative gravities of about 0.02 dex and for 7 K on relative temperatures. The contribution of magnitude difference to the temperature error is therefore very small The contribution of line-to-line scatter is larger for all the pairs (Table 5).

Table 6 shows the sensitivity of the abundance differences to variations of the atmospheric parameters, changing them one-by-one.

Table 7 shows the results of the differential analysis for Fe I and Fe II and Table 8 summarizes the results of temperature difference, metallicity and iron content differences (Fe I from Table 7). We also give the internal errors (due to the line-to-line

Table 5. Temperature difference using different methods. The weighted average between the temperature difference based on the ionization equilibrium of iron and vanadium was adopted because of its higher accuracy.

Object	Ion. Eq. Fe	Ion. Eq. V	Ion. Eq. mean	Exc. Eq.	B-V	V-I	V-K	J-K	J-H	ΔV
HD 8009	371 ± 50	411 ± 36	397 ± 29	408 ± 93	563		649			≤503
HD 8071	24 ± 38	121 ± 36	76 ± 28	234 ± 55	75					≤149
HD 9911	62 ± 33	15 ± 26	32 ± 20	−11 ± 60	–44		14	–39	–149	≤11
HD 13357	267 ± 23	279 ± 16	274 ± 13	279 ± 38	188		272	176	488	≤260
HD 17159	87 ± 21	119 ± 21	104 ± 15	17 ± 49	–54					≤83
HD 19440	198 ± 28	202 ± 37	200 ± 22	282 ± 60	239		339	290	214	≤385
HD 30101	55 ± 17	95 ± 12	82 ± 10	126 ± 27	235	123	34	13	–26	≤73
HD 33334	418 ± 42	470 ± 32	449 ± 26	520 ± 82	295		570	262	489	≤460
HD 66491	9 ± 20	6 ± 12	5 ± 10	21 ± 38	–257		76	277	347	≤32
BD+23 1978	−43 ± 50	−11 ± 43	−25 ± 28	106 ± 224	–142					≤73
HD 106515	98 ± 20	183 ± 13	157 ± 11	206 ± 49	106		174	208	90	≤151
HD 108574/5	307 ± 57	311 ± 45	310 ± 35	392 ± 87	412	322	281	343	215	≤313
HD 123963	399 ± 39	458 ± 31	435 ± 24	539 ± 82	–73					≤422
HD 132563	159 ± 17	209 ± 17	184 ± 12	222 ± 38	108					≤281
HD 132844	72 ± 25	67 ± 19	69 ± 15	36 ± 22	308					≤51
HD 135101	131 ± 27	147 ± 23	140 ± 18	211 ± 60	188	158	136	124	–24	≤472
HD 190042	35 ± 32	97 ± 25	68 ± 20	35 ± 60	220		22	–55	120	≤12
HD 200466	38 ± 41	44 ± 28	50 ± 23	17 ± 92	244		161	236	245	≤77
HIP 104687	87 ± 16	57 ± 13	69 ± 11	53 ± 22	257		6	–163	242	≤25
HD 213013	413 ± 58	412 ± 35	412 ± 35	570 ± 109	315		335	112	203	≤349
HD 215812	121 ± 22	92 ± 19	102 ± 14	124 ± 49	200					≤165
HD 216122	50 ± 42	−27 ± 32	1 ± 26	45 ± 71	–10		237	437	257	≤65
HD 219542	173 ± 12	159 ± 15	168 ± 9	206 ± 27	246	238	232	23	220	≤212

Table 6. Sensitivity to abundance and temperature difference to changes of atmospheric parameters for the pair HD 219542

Changes	Δ FeI	Δ FeII	Δ VI	Δ FeI-FeII	Δ VI-FeII	ΔT_{eff} (Fe)	ΔT_{eff} (V)
ΔT_{eff} +30 K	–0.018±0.008	+0.010±0.013	–0.033±0.024	–0.028±0.016	–0.043±0.027	–32±17	–29±18
ΔT_{eff} –30 K	+0.017±0.008	–0.012±0.013	+0.028±0.024	+0.029±0.016	+0.040±0.027	+32±17	+27±18
Δ log g +0.05 dex	+0.002±0.008	–0.019±0.013	+0.001±0.024	+0.021±0.016	+0.020±0.027	+23±17	+14±18
Δ log g –0.05 dex	–0.008±0.008	+0.020±0.013	+0.000±0.024	–0.028±0.016	–0.020±0.027	–31±17	–13±18
Δ [A/H] +0.05 dex	–0.006±0.008	–0.016±0.013	-0.001±0.024	+0.010±0.016	+0.015±0.027	+11±17	+10±18
Δ [A/H] –0.05 dex	+0.005±0.008	+0.016±0.013	+0.001±0.024	–0.011±0.016	–0.015±0.027	–13±17	–10±18
$\Delta\xi$ +0.15 km/s	+0.017±0.008	+0.030±0.013	+0.005±0.024	–0.013±0.016	–0.025±0.027	–15±17	–17±18
$\Delta\xi$ –0.15 km/s	–0.019±0.008	–0.030±0.013	-0.008±0.024	+0.009±0.016	+0.000±0.027	+11±13	+15±18

scatter) and the global errors that include also the contribution due to the errors on temperature differences. Errors due to microturbulence are not included. The last column of Table 8 lists the estimated amount of iron accreted by the richer in metal component of each pair, derived in Sect. 4.

Our analysis procedure makes use of standard stellar models in the derivation of stellar masses. However, if the outer part of a star is enriched in metals, the model should be systematically wrong. Stellar models with an enriched convective zone have been calculated by e.g. Ford et al. (1999) and Dotter & Chaboyer (2003). In the case of 51 Peg, Ford et al. (1999) found that for a metallicity difference of 0.21 dex, the mass decreases from 1.05 to 0.94 $M_{\odot}$, while for τ Boo Dotter & Chaboyer (2003) found a mass decrease from 1.36 to 1.32 $M_{\odot}$ for the same abundance difference.

We estimated the effects of studing a polluted star with an abundance difference of 0.21 dex using standard models taking as a reference the result by Ford et al. (1999) that predicts a larger effect and is computed for a star with a temperature more typical of the values of our program stars. For fixed magnitudes, the stellar gravity is overestimated by 0.048 dex. This in turn implies an overestimatation of the temperature derived from the ionization equilibrium by about 25 K (with some further effects of the derived stellar gravity) and then a ∼ 0.015 dex overestimatation of the abundance. The induced error is then less than 10% of the real metallicity difference. Since we have not found a pair with a large abundance difference, the impact on our result is very small.

3.3. Comparison with Paper I and other literature data

In Paper I we derived an abundance difference of 0.09 dex for the components of HD 219542, with the primary being more metal rich. The present analysis does not confirm this result.

As described above, we made several modifications of our analysis procedure with respect to Paper I. The continuum

Table 7. Results of differential analysis

Object	Δ [Fe/H]I	rms	N_{lines}	Δ [Fe/H]II	rms	N_{lines}	Δ [V/H]I	rms	N_{lines}
HD 8009	–0.067	0.131	85	-0.090	0.212	25	-0.111	0.152	22
HD 8071	+0.001	0.113	116	-0.046	0.133	17	-0.113	0.151	13
HD 9911	+0.051	0.072	71	+0.078	0.104	13	+0.104	0.108	18
HD 13357	–0.016	0.065	117	-0.022	0.105	27	-0.028	0.072	26
HD 17159	+0.012	0.097	102	-0.004	0.085	28	-0.027	0.095	13
HD 19440	+0.001	0.117	106	+0.002	0.113	25	+0.005	0.202	16
HD 30101	–0.003	0.036	83	-0.028	0.067	20	-0.048	0.040	17
HD 33334	–0.015	0.105	78	-0.042	0.194	29	-0.074	0.161	26
HD 66491	+0.006	0.063	112	+0.010	0.080	22	+0.015	0.030	21
BD+23 1978	–0.012	0.145	43	-0.028	0.135	12	-0.049	0.116	5
HD 106515	+0.018	0.060	75	-0.036	0.075	20	-0.075	0.041	17
HD 108574/5	+0.004	0.160	105	+0.002	0.242	24	+0.000	0.190	17
HD 123963	–0.037	0.137	120	-0.070	0.169	27	-0.105	0.150	20
HD 132563	+0.012	0.090	117	-0.011	0.070	30	-0.049	0.079	13
HD 132844	-0.004	0.052	110	-0.008	0.116	27	-0.005	0.059	13
HD 135101	+0.004	0.116	121	-0.004	0.125	30	-0.013	0.119	24
HD 190042	0.000	0.098	118	-0.030	0.142	26	-0.058	0.129	26
HD 200466	+0.020	0.117	70	+0.009	0.180	28	+0.000	0.111	21
HIP 104687	-0.015	0.045	113	+0.001	0.045	9	+0.018	0.056	19
HD 213013	+0.013	0.123	71	+0.013	0.175	12	+0.012	0.154	15
HD 215812	+0.017	0.092	127	+0.034	0.091	25	+0.050	0.084	22
HD 216122	-0.035	0.145	108	+0.009	0.166	22	+0.051	0.123	14
HD 219542	+0.001	0.057	110	+0.006	0.042	20	+0.012	0.081	23

level and the EWs were re-measured on the same spectra of Paper I to be fully consistent with the other stars studied in this paper, but without significant differences in the EWs with respect to Paper I. We also compared our EWs with those of Sadakane et al. (2003). We obtain a mean difference of -0.050 ± 0.074 mÅ and -0.051 ± 0.069 mÅ with an rms of 3.65 and 3.36 mÅ (24 lines) for HD 219542 A and B respectively.

We performed several tests to understand the origin of the change in abundance and temperature differences with respect to Paper I, introducing one by one the changes between Paper I and this paper, and starting from both the final solution given here and in Paper I. We were able to explain most of the differences in terms of the modifications of the analysis procedure introduced.

The most relevant contributions come from the adoption of different microturbulences for the two stars and for the changes in the formalism for the damping constant (0.02-0.03 dex each one).

The lines selection also plays a role: using the the set of lines of Paper I (limit about 50 mÅ) with the technique used in this paper causes a temperature difference of about 30 K (in the sense of HD 219542B being colder) and then an abundance difference of about 0.02 dex.

Some further minor differences (less than 0.01 dex) are due to the inclusion of vanadium (for this pair the temperature differences based on iron and vanadium differ by just 9 K) and to the changes in the mass determination (inclusion of the metallicity dependence and exclusion of Tycho colors).

The input metallicity used in the analysis also plays a role: when an abundance difference is present between the components, adopting the same abundance difference in the atmospheric parameters causes a further increase of the measured difference. From Table 6 we see that this effect amounts to about 10% of the input difference (i.e. about 0.01 dex for the case of HD 219542 in Paper I).

We also compared our results with those of Sadakane et al. (2003). They used spectra with a higher signal to noise ratio than ours (about 500) but measured a lower number of spectral lines (46 FeI and 7 FeII lines respectively). They determined the atmospheric parameters spectroscopically, fixing the effective temperature and gravity from the excitation and ionization equilibrium respectively. They found (T_{eff}, $\log g$, ξ, [Fe/H]) = (5830,4.45,0.95,0.13) and (5600,4.40,0.90,0.08) for HD 219542 A and B respectively. Our parameters for the primary are fairly similar to their values, while their temperature differences is larger by 62 K. However, we note that the statistical error quoted by Sadakane et al. (2003) for the temperature difference is 42 K (30 K for each star). Furthermore, we note some inconsistencies in the parameters they derived. Their spectroscopic analysis gives gravities larger for the warmer and brighter components ($\Delta \log g(A-B) = 0.05$ dex), contrary to expectation for normal main sequence stars ($\Delta \log g(A-B) = -0.06$ dex from the 1 Gyr isochrone).

As a check that the discrepancy is not due to EW measurements, we analyzed our data using the Sadakane et al. (2003) atmospheric parameters, and found very similar abundance differences than obtained by them, and the Sadakane et al. (2003) EW using our technique. The latter test gives a temperature difference 27 K larger than ours (195 vs 168 K) and an abundance difference of 0.012 dex.

Table 8. Final abundance difference (Fe I from Table 7) and estimates of iron possibly accreted

Object	$\Delta T_{\rm eff(A)}$ K	[Fe/H](A)	Δ [Fe/H]	int. err.	error	ΔM_{Fe} $M_\oplus$
HD 8009	397±30	–0.20	–0.067	0.014	0.029	2.83±1.19
HD 8071	76±28	+0.27	+0.001	0.009	0.021	0.03±0.77
HD 9911	32±20	+0.06	+0.051	0.010	0.019	4.63±1.69
HD 13357	274±13	–0.01	–0.016	0.009	0.013	0.80±0.63
HD 17159	104±15	+0.02	+0.012	0.010	0.016	0.20±0.28
HD 19440	200±22	–0.06	+0.001	0.010	0.022	0.01±0.30
HD 30101	82±11	–0.15	-0.003	0.005	0.010	0.16±0.54
HD 33334	449±26	+0.02	-0.015	0.013	0.025	1.10±1.86
HD 66491	6±10	+0.03	+0.006	0.009	0.011	0.27±0.48
BD+23 1978	-25±28	+0.22	–0.012	0.025	0.032	2.64±7.31
HD 106515	157±11	+0.08	+0.018	0.006	0.012	1.21±0.78
HD 108574/5	310±35	+0.21	+0.004	0.015	0.034	0.10±0.78
HD 123963	435±25	+0.11	–0.037	0.012	0.024	2.50±1.60
HD 132563	184±12	–0.19	+0.012	0.007	0.013	0.12±0.13
HD 132844	69±15	–0.18	–0.004	0.004	0.014	0.06±0.20
HD 135101	140±18	+0.07	+0.004	0.010	0.019	0.20±0.96
HD 190042	68±20	+0.05	0.000	0.010	0.019	0.00±0.96
HD 200466	50±23	+0.05	+0.020	0.012	0.024	0.80±0.97
HIP 104687	69±11	+0.12	–0.015	0.005	0.010	0.49±0.33
HD 213013	412±35	+0.08	+0.013	0.012	0.033	0.86±2.26
HD 215812	102±14	–0.20	+0.017	0.008	0.015	0.31±0.27
HD 216122	1±26	+0.26	-0.035	0.013	0.026	0.99±0.73
HD 219542	168±9	+0.14	+0.001	0.006	0.009	0.03±0.31

While we have no indication that the HD 219542 parallax is inaccurate, we checked the effect on the differential analysis of the adoption of different temperatures for the primary. For differences of 100 K with respect to the adopted values, we get effects on the abundance difference at the 0.01 dex level, likely because the relations between $\log g$ and ξ with T_{eff} are not linear.

The temperature difference adopted in this paper is compatible with the position of the stars in the color-magnitude diagram. The primary might be slightly evolved (about 0.1 mag with respect to the main sequence).

Finally, we note that the analysis of HD 219542B published by Santos et al. (2004) gives (T_{eff}, $\log g$, ξ, [Fe/H]) = (5732,4.40,0.99,0.17), compatible within errors with our estimates.

One may wonder why the results for the other pairs studied in Paper I do not change as did the values for HD 219542 (note that for HD 200466 we use in this paper a new, higher quality spectrum). We think that this is due to the fact that, with the exception of HD 8071, charactrized by a small temperature difference and thus with little effect on the differential analysis, HD 219542 A is the warmest of the stars studied in Paper I. The effect of assumptions about microturbulence (zero for both components in Paper I, different values here) is then largest for this star.

We conclude that the abundance difference between the components of HD 219542 derived in Paper I is likely due the combination of several factors, some random and some systematic, that worked by chance all in the same direction. This signals that caution should be applied when considering abundance differences between pairs of stars, even if they appear to be much larger than the internal errors.

The only other pair for which high resolution spectroscopic analysis is published in the literature is HD 135101, whose components were recently studied individually (i.e. as single stars) by Heiter & Luck (2003). They found (T_{eff}, $\log g$, ξ, [Fe/H]) = (5700,4.20,0.90,0.06 ± 0.04) and (5550,4.24,0.40,0.10 ± 0.05) for HD 135101 A and B respectively. These parameters are fairly similar to ours. From our analysis there is a much larger gravity difference between the components, derived from the magnitude difference (0.85 mag).

4. Results

Fig. 7-9 show the metallicity differences as a function of the temperature difference between the components, the temperature of the primary and that of the secondary. The scatter of abundance difference is larger below 5500 K (Fig. 9). The pattern of Δ [Fe/H] as a function of the temperature of the secondary rensembles that of the difference of temperatures based on iron and vanadium lines but the correlation between Δ [Fe/H] and and $\Delta T_{eff}(Fe-V)$ is not statistically significant.

Four pairs have differences larger than 0.03 dex.

The components of HD 8009 and HD 123963 have a fairly large temperature difference. This causes errors larger than in most cases, making the difference significant to about the 2.5 and 1.5 σ level respectively. The magnitude difference between the components is also quite uncertain for these pairs: the values given by Hipparcos and Tycho differ by more than 0.1 mag

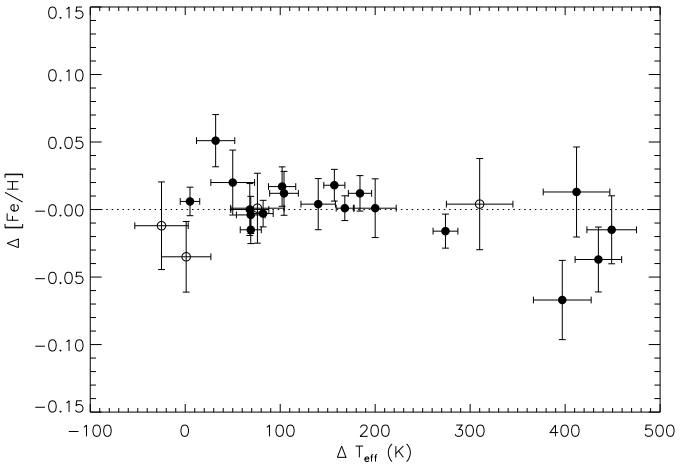

Fig. 7. Iron abundance difference between the components of pairs as a function of temperature difference. Open circles represent stars with rotation broadening larger than about 5 km/s, filled circles slowly rotating stars.

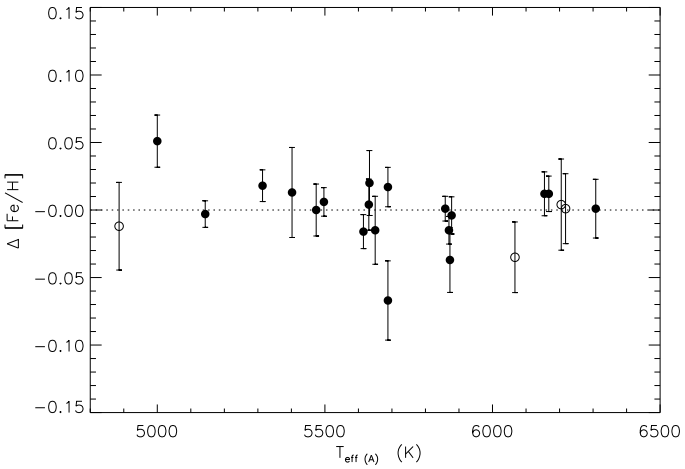

Fig. 8. Iron abundance difference between the components of pairs as a function effective temperature of the primary. Open and filled circles as in Fig. 7.

(see Table 2). The adoption of the Tycho magnitude difference for HD 8009 would imply a decrease of the abundance difference by about 0.01 dex.

The components of HD 9911 are quite cool (with only those of BD+23 1978 being even cooler). We saw that our analysis procedure has some difficulty in handling such stars, likely because of inadequacies of the atmosphere models, so we think the the observed difference (formally significant at about 2.5σ level) is not real.

The components of HD 216122 show significant rotational broadening. As for the other rotating stars, internal errors are larger, making the observed difference of low significance. The star is also listed in the Hipparcos catalog as an unsolved variable.

Thus we have performed a differential abundance analysis of 23 wide binaries, with typical errors of about 0.02 dex. The

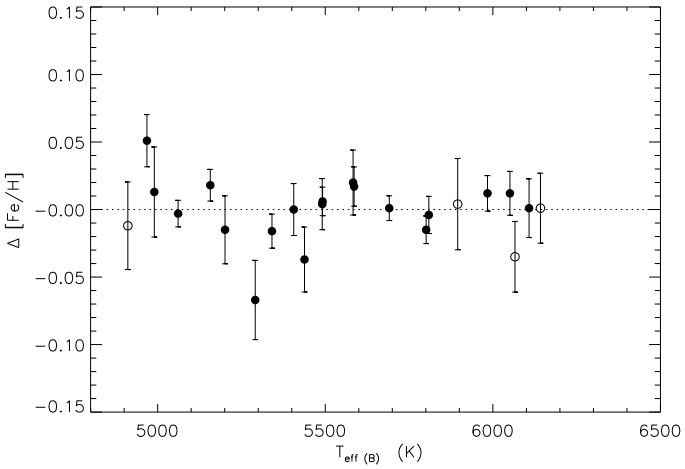

Fig. 9. Iron abundance difference between the components of pairs as a function effective temperature of the secondary. Open and filled circles as in Fig. 7.

analysis appears more robust for the stars warmer than about 5450 K, while some inconsistencies appear to be present for cooler stars. Such warmer stars are also the most interesting for our science goal, because of their thinner convective envelope. While there are some pairs with a marginal abundance difference (0.03-0.07 dex), we take with caution such differences because of possible problems in the analysis of these pairs (errors due to the large temperature difference: HD 123963 and HD 8009; systematic errors of abundance analysis at low temperature: HD 9911), or large random errors, because of the fast rotational velocity (HD 216122).

The analysis of other elements, the search for trends in abundance difference with condensation temperature and the determination of the lithium abundance will be presented elsewhere.

A large fraction of the pairs have abundance differences lower than 0.02 dex. It is possible to estimate rough upper limits on metal-rich material accreted by the stars after their convective zones have shrunk. We follow the approach by Murray et al. (2001). They consider the extension of the convective zone during the main sequence as a function of stellar mass and metallicity. Furthermore, they add a further mixing in the mass range 1.2-1.5 $M_{\odot}$, scaling the amount of mixing according to the observed lithium depletion in this region[7]. We can then calculate the amount of mass of iron that, accreted on the (nominally) metal richer component of each pair, produces the observed abundance difference (Fig. 10).

We are able to exclude at the 1 σ level the consumption of 1 $M_{\oplus}$ of iron for 10 out of 11 slow-rotating stars with stellar temperatures of both components higher than 5400 K. This amount of iron corresponds to less than 5 $M_{\oplus}$ of meteroritic material. The accretion of a quantity of meteoritic material similar to that expected to has been accreted from the Sun after the shrunking of its convective zone (about 0.4 $M_{\oplus}$ of iron, Murray

[7] As noted in Sec. 1, the extra-mixing mechanism producing the Li dip has some dependence on stellar age. This is not taken into account in our estimate of the mass of the mixing zone.

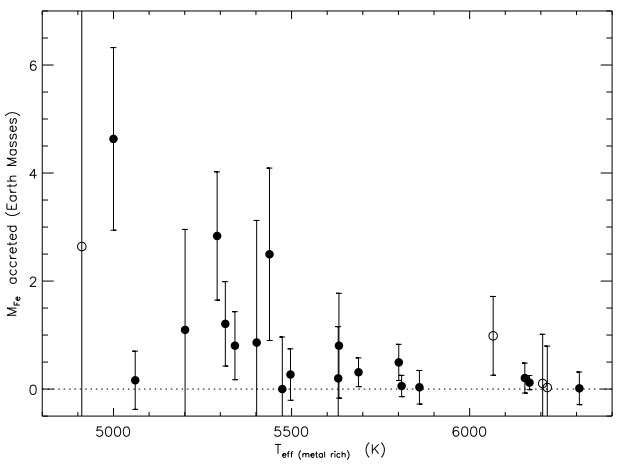

Fig. 10. Estimate of iron accreted by the metal-rich component of each pair as a function of its effective temperature, taking into account the mass of the mixing zone as in Murray et al. (2001). Open and filled circles as in Fig. 7. The mass of meteoritic material is about 5.5 times the mass of iron.

et al. 2001) can be excluded at the 1 σ confidence level in five cases.

A more detailed estimate of the amount of iron accreted by stars of given physical properties requires further investigation of the extension of the mixing zone as well as suitable stellar models with enhanced metallicity in the outer convective zone, that are beyond the scope of this paper. The very small abundance difference of the warmest pairs may also be used to constrain the diffusion of heavy elements within the star. From the models of Turcotte et al. (1998) we see that the effect of iron diffusion at the end of the main sequence lifetime should be of 0.02 and 0.10 dex for a 1.1 and 1.3 $M_{\odot}$ star respectively, i.e. within or close to our detection limit. Such investigations are postponed to a future paper, after the abundance determination of further elements, very useful in constraining the diffusion scenario.

5. Discusssion

The frequency of planets is estimated to be about 8% (Butler et al. 2000) and the stars hosting planets appear to have metallicity larger than 0.25 dex with respect to normal field population stars (Laws et al. 2003). We have not found any pair among 23 with such large composition differences[8]. One star out of 15 in Pleiades might have a metallicity enhancement of about 0.1 dex (Wilden et al. 2002), while two out of 55 in Hyades (with questionable membership) have metallicity difference of about 0.20 dex with respect to the cluster mean (Paulson et al. 2003).

The fraction of stars with metal enrichment comparable to the observed metal overabundance of stars with planets appears to be lower than the fraction of stars with planets. Taken at face value, this indicates that pollution phenomena *alone* cannot explain the planet-metallicity connection. High metallicity then seems to play a role in favouring the presence of planets. Enrichment phenomena might be present, as possibly indicated by the still controversial presence of ^{6}Li in HD 82943, but they should be rare and/or produce only a small composition alteration. Increasing the statistics of wide binaries and stars in clusters in the most suitable temperature range should allow one to constrain the accretion scenario more tightly.

If we consider our sample and those of Pleiades and Hyades, we have 2 possible cases with a metallicity difference comparable to the typical offset between planet hosts and normal field stars (the two Hyades stars) out of 126 stars. With the hypothesis that 8% of these stars have planets (see below for an important caveat) and that the $\sim$ 0.25 dex metallicity offset is entirely due to planetary pollution, we obtain a probability of less than 1% to observe just two cases out of 126 stars. However, such a probability reaches 13% if the actual planet frequency for these stars is 4%.

Some selection effect may be present considering that the temperature and mass distribution of some of the samples studied for the high-precision differential abundance analysis may be different with respect to the field stars selected for radial velocity planet searches.

A more fundamental caveat to this discussion is that the components of wide binaries considered in this study (typical projected separations of about 100-400 AU, Table 1) as well as stars in open clusters like Pleiades and Hyades might have planet frequencies and pollution histories different from the mostly single field star planets hosts. There are some hints that the properties of planets in binary systems are different with respect to those orbiting single stars (Zucker & Mazeh 2002). This seems to indicate a significant role of orbital interactions in the formation and evolution of planetary systems, whose effects on the accretion of planetary material should be considered. Dedicated searches for planets in various kind of binaries (Desidera et al. 2003; Eggenberger et al. 2003) and in star clusters characterized by different dynamical conditions (see e.g. Gilliland et al. 2000; Bruntt et al. 2003; Street et al. 2003; Piotto et al. 2004) are thus very useful to understand the effects of the dynamical environment on the presence of planets and their orbital properties. This will allow us also to determine whether the pollution properties derived by the study of wide pairs and cluster stars can be extended to single stars (for which this is much more difficult to show).

Acknowledgements. We thank the TNG staff for its help with the observations. This research has made use of the SIMBAD database, operated at CDS, Strasbourg, France, and of data products from the Two Micron All Sky Survey, which is a joint project of the University of Massachusetts and the Infrared Processing and Analysis Center/California Institute of Technology, funded by the National Aeronautics and Space Administration and the National Science Foundation.

[8] Considering the observed planet frequency, and the differences of the mass of the convective zone between the components, it appears very unlikely that both components of a binary system have such metal rich material that their original composition is alterated by a similar amount.

References

Alonso A., Arribas S., Martinez-Roger C. 1994, A&AS, 107, 365

Alonso A., Arribas S., Martinez-Roger C. 1996, A&A, 313, 873
Barklem P.S., Piskunov N., O'Mara B.J. 2000, A&AS, 142, 467
Bessell M.S. 1983, PASP, 95, 480
Bessell M.S. 2000, PASP, 112, 961
Boesgaard, A.M.,& Tripicco, M.J. 1986, ApJ, 302, L49
Bragaglia A., Carretta E., Gratton R. et al. 2001, AJ, 121, 327
Bruntt H., Grundahl F., Tingley B., et al. 2003 A&A, 410, 323
Butler R.P., Marcy G.W., Fischer D.A., et al. 2000, in *Planetary Systems in the Universe: Observation, Formation and Evolution*, ASP Conf Series, Penny A.J. et al. eds.
Carney B.W., Latham D.W., Laird J.B., Aguilar L.A. 1994, AJ, 107, 2240
Castelli F., Gratton R.G. & Kurucz R.L. 1997, A&A, 318, 504
Cutri R.M., Skrutskie M.F., Van Dyk S. et al. 2003, Explanatory Supplement to the 2MASS All Sky Data Release (www.ipac.caltech.edu/2mass)
Cuypers J. & Seggewiss W. 1999, A&AS, 139, 425
Desidera S., Gratton R.G., Endl M., et al. 2003, A&A, 405, 207
Docobo J.A., Alvarez C., Lahulla J.F., Lancharesi V., Aguirre A. 2000, Astron. Nachr., 321, 53
Do Nascimento Jr. J.R., Charbonnel C., Lebre A., De Laverny P., De Medeiros J.R. 2000, A&A, 357, 931
Dotter A. & Chaboyer B. 2003, ApJ, 596, 496
Eggenberger A., Udry S. & Mayor M. 2003, in Scientific Frontiers in Research on Extrasolar Planets, ed. D. Deming and S. Seager , ASP Conf. Series 294, p. 43
ESA 1997, The Hipparcos and Tycho Catalogues, ESA SP-1200
Fischer D., Valenti J. & Marcy G.W. 2004, in IAU Symp 219 Stars as Suns: activity, evolution and planets, ed. A.K. Dupree, ASP Conf. Series, in press
Ford E.B., Rasio F.A., Sills A. 1999, ApJ 514, 411
Gilliland R.L., Brown T.M., Guhathakurta P., et al. 2000, ApJ, 545, L47
Girardi L., Bertelli G., Bressan A., et al. 2002 A&A, 391, 195
Gonzalez G. 1997, MNRAS, 285, 403
Gratton R.G. 1988, Rome Obs. Preprint, 29
Gratton R.G. & Sneden C. 1991, A&A, 241, 501
Gratton R.G., Bonanno G., Bruno P., et al. 2001a, Exp. Astron., 12, 107
Gratton R.G., Bonanno G., Claudi R.U., et al. 2001b, A&A, 377, 123 (Paper I)
Gratton R.G., Carretta E., Claudi R.U., Lucatello S., Barbieri M. 2003 A&A, 404, 187
Gratton R.G., Carretta E., Claudi R.U., et al. 2004, Mem SAIt, 75, 97
Gray D.F. 1992, The Observation and Analysis of Stellar Photospheres (Cambridge University Press, Cambridge)
Habing H.J, Dominik C., Jourdain de Muizon M., et al. 2001, A&A, 365, 545
Hanson R.B. 1979, MNRAS, 186, 875
Hauck B. & Mermilliod M. 1998, A&AS, 129, 431
Heiter U. & Luck R.E. 2003, AJ, 126, 201
King J.R., Delyannis C.P., Hiltgen D.D, et al. 1997, AJ, 113, 1871
Kurucz R.L. 1995, CD-ROM 13
Israelian G., Santos N.C., Mayor M. & Rebolo R. 2003, A&A, 405, 753
Laws C. & Gonzalez G. 2001, ApJ, 533, 405
Laws C., Gonzalez G., Walker K.M., et al. 2003, AJ, 125, 2664
Lodders K. 2003, ApJ, 591, 1220
Magain, P. 1984, A&A, 134, 189
Martin E.L., Basri G., Pavlenko Y., Lyubchik Y. 2002, ApJ, 579, 437
Marzari F. & Weidenschilling S.J. 2002, Icarus, 156, 570
Murray N., Chaboyer B., Arras P., Hansen B. & Noyes R.W. 2001, ApJ, 555, 801
Nakos T., Sinachopoulous D., Van Dessel E. 1995, A&AS, 112, 453
Pasquini L., Randich S., Pallavicini R. 1997 A&A, 325, 535
Paulson D., Sneden C., Cochran W.D. 2003, AJ, 125, 3185
Pilachowski C.A., Booth J., Hobbs, L.M. 1987, PASP, 99, 1288
Pinsonneault M.H., De Poy D.L. & Cofee M. 2001, ApJ, 556, L59
Piotto G.P., Montalto M., Desidera S., et al. 2004, in XIXth IAP Colloquium Extrasolar Planets, Today and Tomorrow ASP Conf. Series, in press
Reddy B.E., Lambert D.L., Laws C., Gonzalez G. & Covey K. 2002, MNRAS, 335, 1005
Sadakane K., Ohkubo M. & Honda S. 2003, PASJ, 55, 1005
Sandquist E., Taam R.E., Lin D.N.C & Burkert A. 1998, ApJ 506, L65
Santos N.C., Israelian G., Mayor M. 2004, A&A, 415, 1153
Smith V.V., Cunha K. & Lazzaro D. 2001, AJ, 121, 3207
Street R.A., Horne K., Lister T.A., et al. 2003, MNRAS, 340, 1287
Turcotte S., Richer J., Michaud G. 1998, ApJ, 504, 559
Unsold A. 1955, Physik der Sternatmospharen
Vauclair S. 2004, ApJ, in press (astro-ph 0309790)
Whaling W., Hannaford P., Lowe R.M., Biemont E., Grevesse N. 1985, A&A, 153, 109
Wilden B.S., Jones B.F., Lin D.N.C., Soderblom D.R. 2002, AJ, 124, 2799
Winnick R.A, Demarque P., Basu S., Guenther D.B. 2002, ApJ, 576, 1075
Zucker S. & Mazeh T. 2002, ApJ, 568, L113